Pressure dependence of the boson peak in glasses: Correlated and uncorrelated perturbations

H. R. Schober
Peter Grünberg Institut, Forschungszentrum Jülich, 52425 Jülich, Germany

U. Buchenau
Jülich Center of Neutron Science, Forschungszentrum Jülich, 52425 Jülich, Germany

V. L. Gurevich
A. F. Ioffe Institute, Saint Petersburg 194021, Russia
(Received 6 September 2013; published 27 January 2014)

The pressure dependence of the boson peak in glasses within the framework of the extended soft potential model is reconsidered, taking effects at small pressures into account. One of these is the pressure dependence of the elastic constants, changing the interaction between the soft localized modes and thus changing the quasilocalized vibrations (QLVs) of the boson peak. This and other effects require the introduction of additional parameters to describe all the different influences of the pressure in detail. As in the first treatment of the problem, the dominating high-pressure influence remains the creation of pressure forces, which have to be added to the random forces responsible for the boson peak formation. The pressure forces consist of a correlated and an uncorrelated part (correlated with respect to the already existing random forces). Both lead to the $P^{1/3}$ dependence observed in high-pressure experiments, but the uncorrelated part vanishes at small pressure P. The comparison to experiment is divided into a small pressure part, accessible through low-temperature heat capacity and thermal expansion measurements, and the high-pressure part, mostly Raman scattering measurements of the boson peak under pressure. The results suggest that the latter are dominated by the uncorrelated part of the forces, probably due to pressure-induced relaxations.

DOI: 10.1103/PhysRevB.89.014204 PACS number(s): 63.50.Lm, 65.60.+a

I. INTRODUCTION

One of the characteristic features of glasses is a maximum of the inelastic scattering intensity at low frequencies, typically in the interval of 0.5–2 THz [1] or that of the reduced specific heat $c_p(T)/T^3$. This maximum, the boson peak (BP), can be traced to a maximum of the ratio $g(\omega)/\omega^2$. Here, $g(\omega)$ is the vibrational density of states (VDOS), which itself often has no corresponding maximum. The BP originates from an excess of low-frequency vibrations over the Debye contribution given by the sound waves. Its origin is still disputed. The discussion is confounded by the less than unique definition. Low-frequency maxima in the inelastic scattering intensity are not confined to glassy materials. They are also observed in crystalline structures. This can be due to low lying optic modes or to some acoustic branch being either particularly soft or flattening at low frequencies or dipping at some **q**, e.g., as a precursor of a martensitic phase transition [2]. In these cases, the maximum is an intrinsic property of the crystalline lattice and disorder merely broadens and shifts these maxima. The same holds for low lying optic modes or librations of some molecules in plastic crystals [3–5].

In our work, we are concerned with the case where the BP originates from disorder and is not an intrinsic crystalline effect, broadened by disorder. The importance of disorder for the BP in glassy materials is emphasized by the Ioffe-Regel crossover of the sound waves around the BP frequency ω_b. At long wavelengths, glasses support sound waves—they are, in the continuum limit, isotropic elastic media. With increasing frequency, the sound wave damping increases, the free mean path decreases and drops to the wavelength size (Ioffe-Regel limit) [6]. This may happen somewhere near ω_b (this point is discussed in detail in Ref. [7], section 6). The vibrational states above this limit are no longer propagating modes. Heat transfer, e.g., is more like a diffusive process. The vibrational states have therefore been called diffusons [8]. For completeness, we want to mention that the Ioffe-Regel limit need not be reached for both, longitudinal and transverse, branches at the same frequency. It is even possible that it is not reached at all by the longitudinal branch [9].

A major effort has been spent to describe the BP in terms of random matrix theory for the dynamic matrix [10–12]. These models concentrate on the randomness of the the vibrational coupling constants, in the literature sometimes called elastic constants, that form the dynamic matrix. This means that the random second derivatives of the potential energy are assumed without caring for the random first derivatives (forces) that define the structure. A draw-back of this purely harmonic approach is that some *ad hoc* restrictions are needed to prevent instability, or otherwise some eigenvalues ω^2 turn out to be negative. In nature, stability is restored by the anharmonicity of the atomic interaction. Recently, Beltukov and Parshin presented an inherently stable random matrix model [13]. Since their model does not allow for sound waves, they added an extra term that shifts the modes of the random matrix to higher frequencies and adds sound waves in the gap at the lowest frequencies.

A quite general description of the vibrations in glasses can be given in terms of averaged vibrational Green's functions. The details of disorder effects are subsumed in a self-energy, which is then suitably approximated. In the model of fluctuating elasticity, this is done by concentrating on the low-order terms in an expansion in q space [10,14–16].

Another approach is to relate the structure of the BP vibrations to vibrations of some crystalline counterpart [17,18]. Despite the crossing of the Ioffe-Regel limit near the BP the vibrations are treated as phonons following a dispersion curve. Disorder is assumed to broaden the lowest van-Hove singularities and pull them down to lower frequencies. In particular, this might be by a level repulsion mechanism. In a similar spirit, a softening of the sound velocity at a frequency corresponding to the BP has been invoked [19]. Defining a length scale by $\ell = 2\pi c_t/\omega_b$, with c_t the transverse sound velocity, the boson peak is often related to a spatial correlation [20,21]. However, whatever the origin of the BP, in absence of symmetry, vibrations of similar frequency interact and this correlation therefore does not necessarily indicate the origin of the BP in a structure of size ℓ.

We assume that the BP can be described in terms of quasilocalized vibrations (QLVs) [7,22,23]. The approach is an extension of the soft potential model that successfully describes the low-temperature, low-frequency limit of the vibrational dynamics [24,25]. It generalized the earlier atomic soft potential model [26,27] to more extended modes as seen in experiment [28] and simulation [29]. QLVs occur when positive and negative interatomic force constants almost cancel for some directions in the $3N$-dimensional space of vibrations. Properties of QLVs, also called resonance modes, have been studied extensively for defects, especially interstitial atoms, in crystalline lattices, see, e.g., Refs. [30,31]. For QLVs to be formed, it is not necessary that a single atom is loosely bound to is neighbors, but a group of atoms can collectively have a soft vibrational mode. In simulations, QLVs have been observed while the Einstein spectra, i.e., the single atom vibrations, showed no anomaly [29]. The atoms participating in the QLV also participated in high-frequency modes. A QLV has a material dependent structure, e.g., a coupled libration of tetrahedra in SiO_2 [28] or a chainlike (stringlike) motion in close packed metallic structures [29]. It will always reflect the relative weakness of the local structure of the given substance against some collective motions of groups of atoms. QLVs forming the BP explain the strong sound wave damping observed in experiment [25,32]. Additionally, they explain the nearly universal strength of the two-level systems in glasses [7] as well as the qualitative difference of the diffusion in metallic glasses compared to diffusion in crystals [33]. Our description is in some aspects similar to the one of Klinger whose "soft mode model" [34] also originates from the so-called atomic soft potential model.

Our approach has a strong overlap with those other approaches where the BP is an effect of strong disorder. The harmonic eigenstates which ultimately form the BP are all extended modes and as such they are the eigenmodes of the "random" dynamic matrices. In the long-wavelength limit, the model turns into the one of fluctuating elastic constants [16,32]. For frequencies above the Ioffe-Regel limit, the eigenmodes naturally become diffusons.

In our previous work [7,22], we showed that the interaction of QLVs creates a BP. Due to the lack of symmetry, the interaction between modes at similar frequency causes level repulsion leading to the corresponding density of states $g_{\rm exc}(\omega) \propto \omega$ and a dynamical matrix similar to the one gained in the random matrix models. As in these models, the dynamic matrix shows unstable modes. The underlying physical picture of QLVs allows us to include anharmonicity that stabilizes the system in a nearby configuration. The resulting modified modes can be described in harmonic approximation. They correspond to a "random" dynamic matrix that is restrained to positive eigenvalues. The move from an atomic configuration where some modes are unstable to a nearby minimum where all modes are stable and all eigenvalues of the dynamic matrix are positive, induces forces on all vibrational modes of the original configuration that shift the lowest frequency modes upwards. At low frequencies, the excess spectrum is changed to $g_{\rm exc}(\omega) \propto \omega^4$ [24] and [27]. Together with the level repulsion at higher frequencies the two effects give the BP a universal shape. The BP is essentially described by only two parameters, its position and height. Details, such as the extent of the tail to high frequencies, are material dependent and beyond the simple description. The description is restricted to low frequencies where the specific features of the material, such as peaks in the VDOS are not essential. The influence of the high-frequency modes, though essential, is averaged out and is only summarily included as effect of "high-frequency oscillators." We want to stress that as regards the BP, we treat the vibrations as harmonic.

To gain more insight into the physics of the BP, it is essential to study its dependence on the change of external parameters. The purpose of the present paper is to extend our theory of the boson-peak position ω_b as a function of pressure P. A theory predicting the $\omega_b(P)$ dependence has been worked out by Parshin and two of the authors of the present paper [35]. This theory dealt with the effect of the forces on the QLV, induced by pressure. It predicted a blue shift $\delta\omega_b(P) = \omega_b(P) - \omega_b(0)$ of the BP, sublinear at high pressures, having either the form $\omega_b(P) = \omega_b(0)\,(1 + |P|/P_0)^{1/3}$ or the form $\omega_b(P) = \omega_b(0)[1 + (P/P_0)^2]^{1/6}$—depending on the distribution of the random forces brought about by the pressure variation. These predictions, as regards the high-pressure behavior, were in agreement with previous experiments [36–38] and were confirmed by subsequent experiments [39–43] and simulation [44]. This work concentrated on the effects at high pressures.

In the present work, we include additional smaller effects of pressure, which are essential at low pressure, as seen, e.g., in thermal volume expansion. A change of volume by pressure changes the quadratic terms of the harmonic system of QLV. Both the QLVs eigenfrequencies and their interaction are affected.

Additionally, we correct one point in the theory developed in Ref. [35], namely, the low-pressure behavior of the dominating "uncorrelated" effect. This should always start with a P^2 term rather than with a $|P|$ term, which implies that one does not see the dominating effect in the low-temperature expansion.

In the following, we first recapitulate our model and show the different mechanisms how pressure can affect the BP. In a short excursion, we illustrate how a peak, which is not caused by disorder, is changed by interaction with disorder and finally merges into a "disorder" BP, the subject of the present investigation.

The comparison to experiment shows that our results are able to describe the low-temperature volume expansion of

glasses, though admittedly with more parameters than one can fix by the thermal expansion alone. This is demonstrated for vitreous silica and a polymer. However, for those substances where one has both low-temperature and high-pressure data, the low-temperature effects are always too small to account for the high-pressure behavior in terms of correlated forces. We then discuss what these results and other measurements indicate concerning reversible and irreversible effects and how experiments could clarify this.

II. DENSITY OF STATES

A. The scheme

In this section, we introduce the basic equations and notations that we will need in our analysis. Following Refs. [22,24,35], we exploit the fact that there are low-frequency quasilocalized vibrations (QLVs) in a glass. These QLVs result from the interaction of soft localized modes (SLM) with extended modes (sound waves). The harmonic eigenstates are mixtures of these SLM and the extended modes and are, therefore extended modes. Diagonalizing the dynamic matrix one obtains these eigenmodes where the contribution of the SLM is diluted and not easily observable. In computer simulations, the SLM, in other words QLVs, are directly observed for the lowest frequencies where due to the finite number of atoms the long-wavelength sound waves of similar frequency are cut off [29]. At somewhat higher frequencies, the SLMs can be extracted from the harmonic eigenmodes by a demixing procedure [45]. QLVs are not an artifact of small system sizes. The system size merely determines whether they appear as SLM or are mixed into many eigenmodes and then are seen as low-frequency peaks in the VDOS of some atoms or group of atoms [30,46].

Our description of the boson peak is derived from the properties of the SLM, sometimes briefly called oscillators. As a rule, in glasses, they comprise some ten or even several tens of atoms taking part in a collective vibration. Due to disorder, there will be a distribution of frequencies of such modes that we assume to be smooth and sufficiently broad on the scale of the BP frequency, see also Sec. III. Apart from the textbook example of the heavy substitutional isotope defect, QLVs can result from a weak coupling of an atom or group of atoms to the bulk of the material, e.g., dangling bond modes in open structures, or a weak coupling of some molecular libration. In these cases, the soft-mode frequency directly relates to the atomic coupling to the matrix, the mode frequency $\omega_s \propto \sqrt{f_s}$, where f_s is the coupling constant. These modes will couple weakly to the sound waves. As outlined in Ref. [24], we concentrate on modes resulting from the strong disorder typical for glasses. Since the low frequencies of these modes result from the partial cancellation of positive and negative atomic force constants, small variations of the structure can cause relatively large changes of the vibration frequency resulting in a large spread. The SLMs couple strongly to the sound waves [25]. We denote the spectral density of their squared frequencies by $g_0(\omega^2)$. As in our earlier work [24,25], we expand the potential energy of the single modes in powers of the oscillation amplitude to fourth order from the minimum position:

$$U_i(x) = U_i^0 + M\omega_i^2 x_i^2/2 + B_i x_i^3/3 + A_i x_i^4/4. \quad (2.1)$$

These are the "soft potentials" for the modes. Whereas in Refs. [24,25], the soft potential was written in terms of the displacement of the central atom we use here the notation of Ref. [22], where x stands for the oscillator amplitude. In this notation, the displacement of atom n is given as $\mathbf{s}^n = x\mathbf{e}^n$ with $\mathbf{e}^n$ the harmonic eigenvector of the soft mode. This eigenvector refers to the subsystem of atoms that have a large amplitude, typically ten to hundred atoms. It is not an eigenvector of the total $3N$-dimensional system. There is some arbitrariness in the definition of the subsystem. However, this does not affect the results. An increase in subsystem size is compensated by a reduction in the interaction term. When the subsystem becomes the total system, the interaction between the SLM vanishes and the SLM-eigenvectors become eigenvectors of the total harmonic system. The softness is reflected in the second term of Eq. (2.1). In contrast the anharmonic coefficients A_i are not small, e.g., for silica $A_i \approx 1000\,\mathrm{eV/(nm)^4}$ [24]. This is a typical value of the fourth-order anharmonic constant independent of the smallness of the second-order term. We want to stress that x is a mode coordinate and the translational invariance of the whole system is therefore guaranteed by construction. We assume that due to disorder, there is a broad distribution of frequencies ω_i down to low frequencies $\omega_i \to 0$. Further down, we will briefly discuss the case of a narrow frequency distribution. We have shown previously [35] that the third-order contribution induces a broadening of the the BP but does not shift it significantly. In the following discussion, we will discard this contribution. The interaction of the soft modes with the sound waves induces an interaction between them. We will take this interaction to be weak. (In the case of strongly interacting modes, these would be combined to a pair of split modes with again a weak interaction.) As in the previous papers, we describe the bilinear interaction between modes i and j by an elastic dipole interaction:

$$U_{ij}(x_i, x_j) = I_{ij} x_i x_j \quad (2.2)$$

with

$$I_{ij} = g_{ij} J/r_{ij}^3. \quad (2.3)$$

Here, J is the interaction strength, r_{ij} is the distance between the soft modes and g_{ij} varies in the interval $[-1,1]$. It accounts for the relative orientations of the modes. In the continuum limit, the effect of a defect on the surrounding lattice can be described by the first moment of the forces exerted on the surrounding atoms, the dipole (force) tensor

$$\Pi_{ij} = \sum_n F_i^n r_j^n, \quad (2.4)$$

where n denotes the neighbors of the defect, $\mathbf{F}^n$ is the forces exerted by the defect, and $\mathbf{r}^n$ is the connecting vector [47]. In Ref. [25], we showed, in the context of sound-wave damping, the relation between Π_{ij} and the deformation potentials Λ_l and Λ_t. The interaction energy between two such defined dipoles is in the continuum approximation

$$W^{ab} = \Pi_{ij}^a \Pi_{kl}^b \partial_j \partial_l G_{ik}(r^{ab}), \quad (2.5)$$

where ∂_j denotes the space derivative and $G_{ik}(r)$ is the static elastic Green's function. In using the static Green's function, we neglect retardation effects. Since G decays $\propto 1/r$ the interaction decays with $1/r^3$. The dipole tensors defined in Eq. (2.4) contribute to the energy of the static equilibrium configuration. The change with vibration determines the mode interaction.

The elastic Green's function $G_{ik}(r)$ depends only on distance and sound velocities. For distances comparable to the range of the interatomic interaction, i.e., several nearest-neighbor distances, the interaction should more exactly be written in terms of the interatomic Green's function that is given in terms of all vibrational modes of the glass, not just the long-wavelength ones. This might be important when there is a strong variation of the pressure induced frequency shifts of the modes. For the present, we neglect this additional variation.

We denote the eigenvector of the soft mode σ by $e_j^{(\sigma)n}$ with n denoting the atoms and j standing for x,y,z direction. The dipole tensor then changes in lowest order of the mode amplitude x as

$$\Pi_{ij}^{(\sigma)} = x^{(\sigma)} \sum_n F_i^n e_j^{(\sigma)n}, \tag{2.6}$$

where the sum is over the atoms involved in the soft mode, i.e., twenty to fifty atoms. Together with Eq. (2.5) this determines the interaction term I_{ij} between the modes. The interaction strength depends on the distance and structure of the modes, their relative orientations and on the average the elastic moduli.

The interaction between the modes strongly modifies the low-frequency tail of the spectrum and gives rise to a universal shape of the boson peak in the excess spectrum [22]. The derivation is done in two steps. First, we solve the harmonic problem of interacting modes. The interaction between soft modes and the more numerous higher-frequency modes strongly modifies the original spectrum for $\omega^2 < \omega_c^2$, where ω_c is the so-called limiting frequency, ω_c^2 being proportional to the interaction strength J. The resulting frequency spectrum (VDOS) at low frequencies is linear in ω due to the level repulsion. It extends to negative eigenvalues ω^2. At that stage, our results are similar to the ones of random matrix approximations.

In a second step, the system is stabilized by the anharmonic terms in Eq. (2.1). Taking these terms into account the energy curve for the unstable modes turns into a double well structure with the mode origin at the maximum between the two wells. Stability is restored by displacing the unstable modes into the minima positions where the corresponding eigenvalues are positive.

These displacements are of the order of an interatomic distance. They induce additional dipole forces on all oscillators. Again, the origins of the oscillator modes are slightly shifted and the eigenvalues change due to the anharmonic terms. Whereas for the higher-frequency modes, the frequency shift is negligible the lowest-frequency modes are strongly affected by a blue shift. The excess spectrum at low frequencies goes as $g_{\rm exc}(\omega) \propto \omega^4$, which was found earlier in the soft potential model [24] and is called the seagull singularity. (It is a singularity in the distribution of the stiffness constants of the SLMs in the soft potential model.) It forms the low-frequency flank of the BP. We want to stress again that anharmonicity is an essential ingredient in defining the structure. However, the resulting BP vibrations are harmonic.

We have shown previously that the forces f, acting on the soft modes, have an approximately Lorentzian distribution of width δf:

$$Q(f) = \frac{1}{\pi} \frac{\delta f}{f^2 + \delta f^2}. \tag{2.7}$$

This force distribution is strictly valid for a random distribution of dipoles. The BP frequency is then [7]

$$\omega_b = \sqrt{3} A^{1/6} (\delta f)^{1/3} M^{-1/2}, \tag{2.8}$$

where M and A are the characteristic mass of the oscillators and the fourth-order anharmonicity coefficient, respectively. The power $1/3$ is associated with the fact that it is the fourth-order anharmonicity that stabilizes the system. The pressure dependence of δf was found to be the main contributor to the shift of ω_b at high pressures [7].

B. Pressure effects

1. General considerations

Under an applied external pressure P, the glass will be strained on average by

$$\epsilon_{\alpha\beta} = -(P/3K)\delta_{\alpha\beta} = \epsilon \delta_{\alpha\beta}, \tag{2.9}$$

where K is the compression modulus. On average all distances between atoms will be changed as

$$d_{ij}(\epsilon) = d_{ij}(0)(1+\epsilon). \tag{2.10}$$

Due to disorder in a glass, the displacements will fluctuate. The average displacement is often referred to as affine and the deviations from the average are then separated into random fluctuations around the average and a strongly nonaffine part [48]. Affine and nonaffine distortions are already seen in diatomic crystals without inversion symmetry. There the affine distortion refers to the distortion of the unit cell and the nonaffine one reflects the relative displacement of the two atomic species. Random fluctuations are, of course, absent in such a system. The nonaffine displacements are related to the optical modes. Strong nonaffine displacements are observed also for defects in crystals, e.g., self-interstitials in fcc metals where they are related to QLVs of the interstitial atoms [31]. We believe that the nonaffine displacements in glasses are related to the BP, i.e., the soft modes. Due to the large effective mass of the SLMs [24], they are correlated over some length. The random fluctuations, on the other hand, vary on an atomic scale and we will treat them as uncorrelated to the soft modes. The change of the parameters of the expansion (2.1) and (2.2) is twofold. The parameters will on average both be shifted with strain ϵ and gain additional fluctuating contributions:

$$\omega_i^2 \to \omega_i^2 + \overline{\delta\omega_i^2}\epsilon + \left(\delta\omega_i^2 - \overline{\delta\omega_i^2}\right)\epsilon, \tag{2.11}$$

$$A_i \to A_i + \overline{\delta A_i}\epsilon + (\delta A_i - \overline{\delta A_i})\epsilon, \tag{2.12}$$

$$I_{ij} \to I_{ij} + \overline{\delta I_{ij}}\epsilon + (\delta I_{ij} - \overline{\delta I_{ij}})\epsilon. \tag{2.13}$$

Here, the bar denotes averaging over soft modes within some frequency interval $\Delta\omega$ much smaller than the average eigenfrequency of the QLVs.

In our model, the shape of the excess intensity is not changed markedly by pressure. The change of strength of the low-frequency ω^4 contribution shifts the position of the maximum, the boson-peak frequency ω_b, and concomitantly the intensity $g_{\rm exc}(\omega_b)$ varies. Modes shifted from/into the low-frequency part are compensated in the high-frequency tail of the BP ($\omega_b < \omega < \omega_c$). For low pressure, in linear approximation, the pressure effect can be expressed in terms of two effective Grüneisen constants:

$$\omega_b(P) = \omega_b(0)(1 + \Gamma_b P/K), \tag{2.14}$$

$$g_{\rm exc}(\omega_b, p) = g_{\rm exc}(0)(1 + \Gamma_g P/K). \tag{2.15}$$

In the following, we show how both affine and nonaffine distortions contribute to the two parameters. Increasing the pressure, we believe that eventually the nonaffine effects will dominate. These lead to the asymptotic pressure dependence with $P^{1/3}$ discussed in the previous work [35]. We show that the main contribution is from two effects, which we denote as correlated and uncorrelated. For positive pressures, the two contributions are additive (provided the signs of the coefficients describing their pressure dependence are the same), whereas for negative pressures their difference enters.

2. *Affine effects*

A special case and the most straightforward assumption would be that all modes comprising the BP shift by a common factor $\omega(P) = \omega(P = 0)(1 + \gamma_G P/K)$. The BP frequency then changes with the same factor:

$$\omega_b(P) \approx \omega_b(0)(1 + \gamma_G P/K), \tag{2.16}$$

and the excess intensity at the BP changes, due to the stretching of the VDOS and the denominator ω_b^2, with the third power:

$$\frac{g_{\rm exc}(\omega_b, P)}{\omega_b^2(P)} = \frac{g_{\rm exc}(\omega_b, P = 0)}{\omega_b^2(p = 0)} \frac{1}{(1 + \gamma_G P/K)^3}. \tag{2.17}$$

Here, γ_G is the average mode Grüneisen constant, defined as $\gamma_G = -\overline{d(\ln\omega)/d(\ln V)}$.

Assuming further that the Grüneisen constant of the excess modes equals the one of the sound waves, one gets $g_{\rm exc}(\omega, P)/g_{\rm Debye}(P) = {\rm const}$ for $\omega \lesssim \omega_b$. This simple case is given if all interatomic interactions scale with a common single parameter. For a purely repulsive soft sphere interaction $1/r^n$, this case was treated recently [49]. The resulting scaling laws reflect then the scaling of energy with distance. As the authors state, in nature, this might apply to systems under extremely high pressure when the physics is determined fully by the nearest-neighbor repulsion and the attractive interaction has a negligible contribution. This special case is outside the scope of the present work.

Equations (2.1) to (2.3) determine the BP essentially by the spectrum of noninteracting soft modes ω_i and their interaction I_{ij}. The frequencies ω_i are determined by local configurations of atoms causing near instabilities. The strength of the interaction, on the other hand, depends not only on the local geometries but also on the average elastic coefficients of the glass matrix. Our description in terms of QLVs thus provides a richer scenario. Two "partial Grüneisen parameters" emerge in our theory: one describes the shift of the noninteracting local modes

$$\omega_i(P) = \omega_i(P = 0)(1 + \gamma_\omega P/K) \tag{2.18}$$

and a second one the change of the interaction strength

$$I(P) = I(P = 0)(1 + \gamma_J P/K)^2 \approx I(P = 0)(1 + 2\gamma_J P/K). \tag{2.19}$$

Here, we introduced the factor $(1 + \gamma_J P/K)^2$ because it refers to an energy term instead of a frequency term. A change of the fourth-order term Eq. (2.1) with pressure changes ω_b only negligibly. Not too large changes of the third-order term slightly broaden the BP excess density of states [22,35].

The shift of the BP frequency when the interaction strength changes, whereas the frequencies ω_i, of the noninteracting modes are kept constant, was given earlier [22] as

$$\omega_b(P) = \omega_b(0)(1 + \gamma_J\ P/K)^{2+2n/3}. \tag{2.20}$$

Here, n denotes the slope of $\log g(\omega)$ in the vicinity of the limiting frequency ω_c below which the interaction will create unstable modes. To keep in line with the definition of the Grüneisen parameter, we write here, different from the previous reference, the change of the interaction strength J quadratic in γ_J. In general, the interaction term changes with pressure both due to a change of stiffness of the glass and the reduction of the distances between soft mode centers. If the variation of the mode Grüneisen parameters of the modes responsible for the interaction is not too large, one can write approximately

$$\gamma_J \approx 0.5 - \gamma_D. \tag{2.21}$$

Here, the first term reflects the increase of the interaction when the distances between the modes change due to a volume reduction by pressure. The second term accounts for the reduced interaction when the elastic moduli increase, Eq. (2.3). The interaction strength J is inversely proportional to an elastic modulus. We show further down that this approximation can be used in the cases of polymethylmethacrylate (PMMA) and silica.

In the opposite case, $\gamma_J = 0$, we get from Ref. [22] Eq. (26):

$$\omega_b(P) = \omega_b(0)(1 + \gamma_\omega\ P/K)^{-1-2n/3}. \tag{2.22}$$

Surprisingly, keeping the interaction constant, hardening of the noninteracting soft modes with pressure is concomitant with a softening of the BP frequency ω_b. The reason for this is that hardening of the noninteracting soft modes reduces the number of modes that are sufficiently affected by the mode-mode interaction to form a BP (the equation assumes the same γ_ω for all modes participating in the creation of the boson peak, in particular, those which are instable and get stabilized by the fourth-order term).

Combining the two terms, the shift of the BP in this approximation becomes

$$\omega_b(P) = \omega_b(0)(1 + \gamma_J\ P/K)^{2+2n/3}/(1 + \gamma_\omega\ P/K)^{1+2n/3}. \tag{2.23}$$

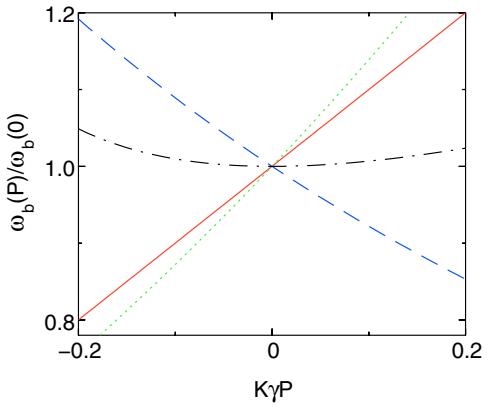

FIG. 1. (Color online) Shift of the BP frequency for different Grüneisen constants for a typical value $n = 1$. Solid red line: $\gamma_J = \gamma_\omega = \gamma$, dashed blue line: $\gamma_J = 0$, $\gamma_\omega = 0.5\gamma$, green dotted line: $\gamma_J = 0.5\gamma$, $\gamma_\omega = 0$, and black dash-dotted line: $\gamma_J = \gamma$, $\gamma_\omega = 1.6\gamma$.

In the case $\gamma_J = \gamma_\omega$, this reduces to the simple result Eq. (2.16). In the general case, the BP frequency can, depending on the strengths of γ_J and γ_ω, with pressure increase or decrease or even go through a minimum. Figure 1 depicts this variation for different scenarios. The approximate shape of the BP excess DOS {Eq. (27) in Ref. [22]} can be used to estimate the change of the VDOS at the BP:

$$g_{\rm exc}(\omega_b, P) = g\,(\omega_b, P = 0)\,\frac{(1+\gamma_J\,P/K)^{8n/3}}{(1+\gamma_\omega\,P/K)^{1+8n/3}}. \quad (2.24)$$

Again, one sees the competing effects of the two variations. For the simple case $\gamma_J = \gamma_\omega$, the BP intensity decreases with $(1+\gamma\,P/K)^{-3}$, whereas, in general, the intensity depends on the underlying atomic mechanism both through the ratio γ_J/γ_ω and the DOS of the noninteracting modes, in our simplified description the value n.

For the above estimates, the VDOS of the BP was approximated by ω^4 and ω dependencies below and above ω_b, respectively. More exact values can be obtained numerically. In Fig. 2, we show, for the case $\gamma_\omega = 0$ how the BP intensity

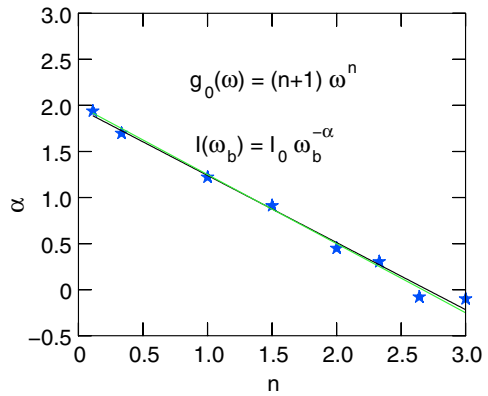

FIG. 2. (Color online) Dependence of the BP intensity on the BP frequency under a change of the interaction strength. Symbols: numeric calculation, black line: least square fit, and green line: $\alpha = 2 - 0.75n$.

changes with the shift of the BP. It can be described by a simple dependency

$$I(\omega_b) = I_0{\omega_b}^{-2+0.75n}. \quad (2.25)$$

The decrease with increasing ω_b is always less than the ω_b^{-3} found for the simple overall Grüneisen scaling. The effective logarithmic slope n of the DOS of the noninteracting modes is a parameter in our general description. Hopefully, experiments on systems where the atomistics is understood will provide some information in future. To verify the analytic results, we repeated the previous numerical simulation of our equations [22] for different values of n. The simulations were done for samples of 2197 oscillators placed on a simple cubic lattice with periodic boundary conditions. The interaction was changed by varying J. The lattice parameter was kept constant, the $g_{i,j}$ were random numbers from the interval $[-1,1]$, independent of J. The anharmonicity parameters were kept constant, $B_i = 0$ and $A_i = 1$. Within numerical accuracy we did not see a deviation from the analytic results.

Little is known about n, which mimics the frequency dependence of the VDOS of the noninteracting soft modes. It will probably be not too far from $n = 1$ or $n = 2$, which we shall assume for the fits to experiment further down. This leaves then again two parameters. If Eq. (2.21) holds, one is left with a single parameter. We will show further down that the reduction to a single parameter suffices to reproduce the experimentally observed low-temperature thermal expansion of vitreous SiO_2 and PMMA.

3. *Nonaffine effects: uncorrelated forces*

In our previous work, we have dealt with the shift of the BP due to forces induced by pressure. This shift is additional to the one treated above. We begin with a discussion of the uncorrelated part of the QLV-strain interaction. Not repeating the derivation of Ref. [35], we will discuss some of its crucial points. The interaction between the strain and a soft oscillator is bilinear:

$$\mathcal{H}_{\rm int} = \sum_{i,k} \Lambda_{ik}\varepsilon_{ik}x, \quad (2.26)$$

where Λ_{ik} is the deformation potential tensor and x is the coordinate of the QLV. As we have shown in our earlier work, the interaction between the soft modes and the subsequent stabilization introduces random forces f on the modes [7,22]. The deformation by pressure adds additional forces Δf [35]. The total random force $\widetilde{f}$ has then two contributions

$$\widetilde{f} = f + \Delta f. \quad (2.27)$$

To find the correlation function of the static random forces acting on the QLVs, one should sum over all the neighboring two-well configurations. The random force Eq. (2.27) is linear in the deformation potential Λ and can be expressed via its angular average components

$$\overline{\Lambda}_{xx} = \overline{\Lambda}_{yy} = \overline{\Lambda}_{zz} \equiv \tfrac{1}{3}\overline{\Lambda}. \quad (2.28)$$

If the distribution of the random forces at $P = 0$ is $Q(f)$, then the distribution of the total random force $\widetilde{f}$ at some

pressure P is given by the convolution

$$F_P(\tilde{f}) = \int_{-\infty}^{\infty} Q\left(\tilde{f} - \frac{P}{3K}\bar{\Lambda}\right) D(\bar{\Lambda}) d\bar{\Lambda}. \quad (2.29)$$

Here, $Q(f)$, given by Eq. (2.7), is the distribution of random forces in the absence of pressure—see Ref. [22]—while $D(\bar{\Lambda})$ is the distribution of the values of the deformation potential averaged over the "directions" of the QLVs.

As reported earlier, the shift of the BP by the additional forces for large pressures is given by

$$\omega_b(P) = \omega_b(0)(1 + |P|/P_0)^{1/3} \quad \text{for } |P| \gtrsim P_0, \quad (2.30)$$

where P_0 is a material dependent parameter. It can be expressed approximately in terms of the bulk modulus and the deformation potential as $P_0 = 3Kf_0/\Lambda_0$ [35] where all quantities refer to the $P = 0$ state and f_0 is a material parameter. Since changes of the bulk modulus and the deformation potential with increasing pressure largely cancel, Eq. (2.30) can remain valid for materials with marked hardening under pressure. This has been observed in experiment [40]. The extra forces enhance the strength of the seagull singularity—the low-frequency ω^4 flank is extended to higher frequencies. The total number of SLM is not markedly changed. Consequently, the excess intensity at the BP changes to

$$g_{\text{exc}}(\omega_b, P)/\omega_b(P)^2 \propto \omega_b(P)^{-1}. \quad (2.31)$$

Such a dependence has been observed by Andrikopoulos *et al.* [39] in As_2S_3 at room temperature.

Though the experiment seems to corroborate Eq. (2.30) even down to low pressure, one can show that in the low-pressure limit the approximation must break down. For small values of P ($P \ll P_0$), one can expand Eq. (2.29) and get [as $\int_{-\infty}^{\infty} d\Lambda\, D(\Lambda) = 1$]

$$F_P(\tilde{f}) = Q(\tilde{f}) + \frac{1}{2}Q''(\tilde{f}) \int_{-\infty}^{\infty} d\Lambda\, D(\Lambda)\Lambda^2 \left(\frac{P}{3K}\right)^2, \quad (2.32)$$

where the linear term vanishes since $D(\Lambda)$ is an even function of Λ. This vanishing of the linear term was also seen in the simulation of our model, see Fig. 4 in Ref. [35]. The pressure-induced additional forces, which are uncorrelated to the forces creating the BP thus do not contribute to the low-temperature expansion, which we discuss further down in this paper.

The approach is based on two assumptions. First, we assume that there is no correlation between the functions $Q(f)$ and $D(\bar{\Lambda})$. Indeed, the random forces f are due to the action of neighboring two-well configurations on a particular QLV. They depend not only on the deformation potential of the QLV but also on deformation potentials of the two-well configurations. This is a random quantity. The second assumption is that the pressure does not induce a transition to a different glass structure. The latter assumption does not preclude a limited number of local configurational changes taking the glass to some configuration which is metastable at $P = 0$. Reversibility then depends on temperature.

In this reasoning, one point is left out, namely, the special role of the "initial" pressure $P = 0$. We have implied that the glass is grown out of a melt (in other words, quenched) at $P = 0$. Had it been grown at some external pressure P_1 the situation would have been more involved as a "memory" of P_1 would be preserved within the glass. It is worthwhile to note that the same situation could emerge provided the glass is grown, for instance, in an external dc electric field $\mathbf{E}$. The "equilibrium" state of the glass after cooling down would then be characterized by the vector $\mathbf{E}$.

4. *Nonaffine effects: correlated forces*

Leonforte *et al.* [48] report for a Lennard-Jones glass nonaffine displacements with correlation lengths of some 20 nearest-neighbor distances. These nonaffine regions correlate with the excess BP modes. This finding can be understood from the properties of QLVs. As shown in Ref. [24] the soft modes extend over 20 to 100 atoms or molecular units. Furthermore the soft modes tend to cluster. Particularly large nonaffine displacements occur in the presence of soft (quasi) localized modes. This can easily be understood considering that in an harmonic system the static response function of an eigenmode to an external force, $\mathbf{f}^n$ can be written as

$$g_{ij}^{(\sigma)nn'} = \frac{e_i^{(\sigma)n} e_j^{(\sigma)n'}}{m^\sigma \omega^{(\sigma)2}}, \quad (2.33)$$

which means the displacement of an atom participating in a mode is the larger the more localized the mode and the lower its frequency. This effect is well known in the physics of crystalline defects, e.g., interstitial atoms in fcc metals [31].

Large nonaffine displacements indicate a strong coupling of some modes to strain. This will lead to changes of both the frequencies ω_i of the noninteracting modes and of their interaction. They will be more pronounced the lower the frequency. The sign and magnitude of this change will depend on the type of glass. A much larger effect is expected from the change of forces. We have seen above that the static forces due to the stabilization of the modes, i.e., the change of the origin in a double well potential, create the sea-gull singularity and are responsible for the BP.

Strain induces an additional dipolar effect Π_{ij}^{ind}, which can be written in terms of a polarizability matrix

$$\Pi_{ij}^{\text{ind}} = \sum_{kl} \alpha_{ijkl}\epsilon_{kl}, \quad (2.34)$$

where α_{ijkl} is the (dielastic) elastic polarizability [31]. For a given defect concentration, this polarizability reduces also the average elastic moduli

$$\Delta C_{ijkl} = -\frac{c}{v_a}\alpha_{ijkl}. \quad (2.35)$$

The polarizability of a low-frequency QLV can be quite large. For an order of magnitude estimate, we take the polarizability of an interstitial defect in crystalline Cu [50]:

$$\frac{\Delta\Pi}{\mu} \approx 100 \text{ eV}, \quad (2.36)$$

where μ is the distortion strength. The above value depends strongly on the local geometry of the distortion and there might be a large variation between different materials. For a pressure of $P = 1$ GPa and the bulk modulus of Cu $B = 140$ GPa, this gives an estimate of $\Delta\Pi_{ij} \approx \delta_{ij}(-0.4 \text{ eV})$. This is comparable to the typical values around 1 eV for the active parts of the

dipole tensor [25]. We have to remember, however, that the mode interaction is not determined by the total dipole tensor but only by the part that couples to the given mode. This can, depending on the structure of the glass, reduce the effect of a given strain.

We can now consider the shift of δf due to pressure. Making use of the equation (see Ref. [7])

$$\delta f = D\left(\frac{M^3}{A}\right)^{1/2}\omega_c^3\left(\frac{\omega_c}{\omega_0}\right)^n, \tag{2.37}$$

one can write for the variation of $\Delta(\delta f)$ with pressure

$$\Delta(\delta f) = \left[-\frac{1}{2}\frac{\Delta A}{A} + (3+n)\frac{\Delta\omega_c}{\omega_c} - n\frac{\Delta\omega_0}{\omega_0}\right]\delta f, \tag{2.38}$$

where D is a constant of order of unity and ω_0 is a limiting frequency, typically about the Debye frequency. We will consider such pressures that the strain $|\epsilon| \ll 1$. Then in the first approximation, assuming that A, ω_c, and ω_0 are continuous functions of strain, one can write for the variation of these quantities under pressure:

$$\frac{\Delta A}{A} = \gamma_A\epsilon, \quad \frac{\Delta\omega_c}{\omega_c} = \gamma_c\epsilon, \quad \frac{\Delta\omega_0}{\omega_0} = \gamma_0\epsilon, \tag{2.39}$$

where γ_A, γ_c, and γ_0, are dimensionless constants. Their absolute values are of order of (or a little bigger than) unity. As a result, one gets

$$\Delta(\delta f) = \gamma\epsilon, \quad \text{where} \quad \gamma = -\gamma_A/2 + (3+n)\gamma_c - n\gamma_0. \tag{2.40}$$

Due to polarization, the forces exerted by the two-well configurations will thus be multiplied on average by a factor $(1+\alpha_{\rm corr}P)$, so that

$$\tilde{f}(P) = f(1+\alpha_{\rm corr}P), \tag{2.41}$$

where $\alpha_{\rm corr} = -\gamma/K$. Consequently, the width of the force distribution will be multiplied by the same factor and, only taking this effect into account, the BP frequency shifts as

$$\omega_b(P) = \omega_b(0)(1+\alpha_{\rm corr}P)^{1/3}. \tag{2.42}$$

For $\alpha_{\rm corr} > 0$ and positive pressures, this corresponds to our earlier result but shows an inverse effect for negative pressures (or positive pressures and $\alpha_{\rm corr} < 0$).

Together with Eq. (2.30), the total shift due to the correlated and uncorrelated forces is for high pressures,

$$\omega_b(P) = \omega_b(0)\left(\sqrt{1+\alpha_{\rm uncorr}^2P^2} + \alpha_{\rm corr}P\right)^{1/3}. \tag{2.43}$$

Writing $\sqrt{1+\alpha_{\rm uncorr}^2P^2}$ interpolates the pressure dependence for intermediate pressures and is exact (analytical) for the limiting cases of low and high pressures. There is no quantitative theory for intermediate pressures as one does not know the random properties of the deformation potential. In the low-pressure limit, the correlated contribution vanishes linearly unlike the uncorrelated effect. In contrast to this, the correlated contribution persists and thus contributes to the thermal expansion, discussed below. Setting $\alpha_{\rm corr} + \alpha_{\rm uncorr} = 1/P_0$, the form of our previous result may be regained for $|P| \gg P_0$.

5. *Relaxations and permanent densification*

So far, we have dealt with changes of the VDOS not involving relaxations, the diaelastic effects. Double well potentials are, however, tantamount to the existence of paraelastic effects. Under an applied external pressure, the equilibrium occupation probability of the minima changes. Equilibrium is restored by relaxations over the separating barrier. These local changes will induce additional forces on all soft modes and will give an additive contribution to $\alpha_{\rm uncorr}$.

Above the tunneling regime, relaxation is a phonon activated process with a temperature dependent time constant. In a glass, one expects a continuum of such relaxation times. At finite temperatures, transitions between the minima of some two well systems with a comparatively low barrier will be rapid and merge with the diaelastic contribution. However, there is an increasing number of relaxations with higher and higher barriers, ending only at the effective barrier height of the flow process of about $30\,kT_g$, where T_g is the glass temperature. So one has to reckon with a large number of possible relaxations with barriers of the order of 1 eV.

While usually these very high barriers play no role in the glass, the situation changes at high pressures, where one changes the volume of the glass by a sizable percentage. It is to be expected that the coupling constant of these high barriers to the external compression is markedly higher than the coupling constant of the low-barrier tunneling states, which is known to be of the order of 1 eV. Consequently, some of the high barriers are lowered to half their low-pressure value or even less by the high pressure and can be jumped over at the lower temperature. Taking the pressure away again, the sample can remain in a minimum with a smaller volume, which was not accessible at low pressure, and thus remain permanently densified. The permanent densification is the compression counterpart of the plastic deformation under a large shear. Since the local density change is much larger than the overall one, the densification is still a sum of relatively few local processes, which leaves the rest of the sample essentially the same, though in a slightly more strained state. Again, such a local change will induce additional forces on all soft modes and will give an additive contribution to $\alpha_{\rm uncorr}$ in the densified sample. In the comparison to experiment, we will discuss the example of densified silica.

III. OTHER BOSON PEAKS

There is no generally accepted definition of boson peak. The boson peak, we discussed so far, we will briefly call *soft potential BP*, the corresponding physics is put forward in detail in our papers [7,22]. As mentioned in the introduction, low-frequency maxima of the scattering intensity can have many different origins. We consider a broad distribution of soft modes that are caused by disorder. The structure of these soft modes might well resemble fragments of a low-frequency optical mode, as argued, e.g., for vitreous silica [3]. The situation is different for soft modes such as librating molecules in plastic crystals [4,5]. These modes will have a well-defined

frequency that is broadened by disorder. Such a peak might show a different behavior depending on broadening and interaction. For weak interaction, the pressure effect on these modes is dominated by their local structure. For sufficiently strong interaction, these modes will behave as discussed in this paper. To simulate this schematically, we used again the simulation scheme of our previous work [22]. The spectrum of the noninteracting modes consisted of two parts. 95% of the modes were distributed according to $g_0(\omega) = 1.9(\omega - 0.25)$ for $0.25 < \omega < 1.25$ and zero otherwise. To this, we added a narrow Gaussian distribution of modes amounting to 5% centered at $\omega = 0.25$ with variance 0.01. With this distribution, we solved numerically the equations (2.1) with the interaction term (2.2). For simplicity, we set $B_i = 0$ and $A_i = 1$. The simulation was done for samples of 2197 oscillators, placed on a simple cubic lattice with periodic boundary conditions. Disorder was simulated by varying g_{ij} randomly in the interval $[-1,1]$. For each coupling strength, at least 25 000 samples were calculated. The effect of a change of the coupling strength J, Eq. (2.3), is shown in Fig. 3. For not too large couplings ($J < 0.10$), as to be expected, the Gaussian line broadens and shifts to slightly lower frequencies. More interesting is the evolution of a shoulder on the low-frequency flank ($J = 0.07$) that evolves for $J = 0.10$ into a secondary peak. This secondary peak is the "boson peak" discussed in our work. Increasing the coupling even more, the two peaks merge and for $J = 0.20$ only a single boson peak remains.To illustrate this anomalous behavior, we show in Fig. 4 the shift of the intensity peaks against coupling. Increasing J, we observe a weak red shift of the Gaussian peak. In contrast, the (disorder-)boson peak shows the blue shift expected from our work. The theory presented in this paper is valid only for the lower branch. It describes the shift of the low-frequency peak caused by disorder. To accurately describe the shift of the original peak, upper line in Fig. 4, the model would have to be extended to include the shape of the original peak. Note that Figs. 3 and 4 were calculated under the assumption the frequencies of the noninteracting modes do not change under pressure, $\gamma_\omega = 0$.

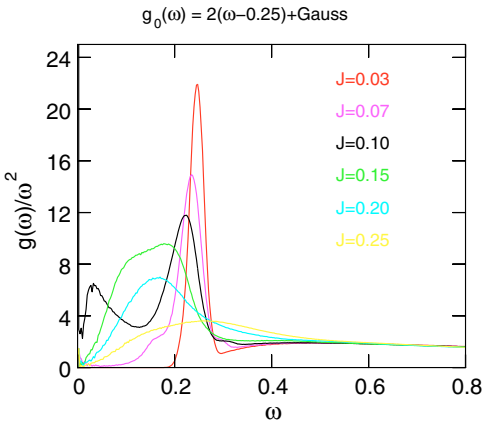

FIG. 3. (Color online) Excess mode density for a Gaussian distribution of modes coupled to a small density of modes with frequencies $\omega < 0.25$. The coupling strength between modes (2.3) is varied from $J = 0.03$ to 0.30. The decay of the intensity of the Gaussian peak near $\omega = 0.25$ follows the increase of the coupling strength J.

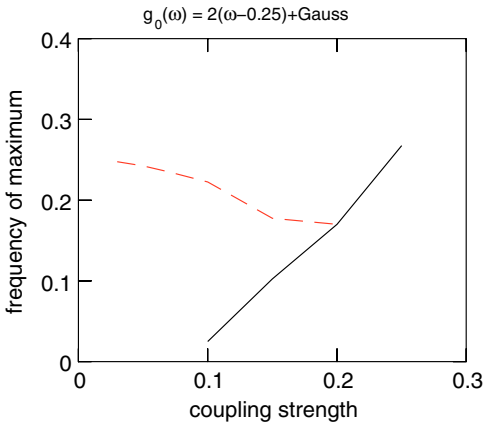

FIG. 4. (Color online) Evolution of the maxima of the reduced excess VDOS, Fig. 3, as a function of coupling strength (red dashed line: Gaussian modes, and black solid line: disorder).

IV. COMPARISON TO EXPERIMENT

A. Thermal volume expansion

One of the questions raised in the present paper is whether our model, which is able to explain the measured high-pressure boson-peak shifts, is also able to explain the boson-peak shift at low pressure. In order to answer this question, one needs an accurate determination of the boson-peak shift at low pressure.

Such an accurate determination of the low-pressure boson-peak shift is possible using the heat capacity per unit volume $c_P(T)$ and the thermal volume expansion $\alpha(T)$ of the glass at low temperature. In the heat capacity, the boson peak is manifest as a maximum in c_P/T^3 at a temperature $T_{\max}$ of about 5 to 10 K. One can define a temperature-dependent Grüneisen parameter $\Gamma(T)$ by the Grüneisen relation

$$\Gamma(T) = \frac{\alpha(T)K}{c_V(T)} \tag{4.1}$$

[note that at these low temperatures, the heat capacities $c_P(T)$ and $c_V(T)$ are practically identical].

In the simplest possible approximation, one can identify the Grüneisen parameter Γ_b of the boson-peak frequency with $\Gamma(T_{\max})$:

$$\Gamma(T_{\max}) = \Gamma_b = \frac{\partial \ln \omega_b}{\partial \ln V}. \tag{4.2}$$

This approximation holds if all modes in the neighborhood of the boson peak have the same Grüneisen parameter. In experiment, this can be immediately seen by an essentially constant $\Gamma(T)$ in the region around $T_{\max}$. We will later discuss an example (PMMA) showing this behavior. It can be recognized experimentally already by the peak in $\alpha(T)/T^3$, which for a mode-independent Grüneisen parameter appears at the same $T_{\max}$ as the peak in c_P/T^3. In such a case, the intensity $g(\omega_b)/\omega_b^2$ changes with $1/\omega_b^3$, as discussed in the context of Eq. (2.16).

If the Grüneisen parameter is not the same for all modes in the boson-peak region, the low-temperature thermal volume expansion coefficient $\alpha(T)$ is obtained by a sum over all low-frequency modes. The resulting Grüneisen parameter $\Gamma(T)$ can be written in terms of the Grüneisen constants Γ_i of the

single modes as [51]

$$\Gamma(T) = \frac{\sum_i \Gamma_i c_{iV(T)}}{\sum_i c_{iV(T)}}, \tag{4.3}$$

where the sum is over all vibrational modes and $c_{iV(T)}$ is the contribution of mode i to the heat capacity at the temperature T:

$$c_{iV(T)} = k\left(\frac{\hbar\omega_i}{2kT}\right)^2 \Big/ \sinh^2(\hbar\omega_i/2kT) \tag{4.4}$$

with k the Boltzmann constant. Depending on the material, there can be a considerable variation in the Γ_i values. They can even vary in sign. In our examples, vitreous silica will turn out to be a case where the peak in $\alpha(T)/T^3$ is markedly shifted with respect to $T_{\max}$, so one needs to take the frequency variation of the Grüneisen parameter explicitly into account. This implies a scaling of $g(\omega_b)/\omega_b^2$ with ω_b^{-a}, where a is not equal to 3.

Having determined the correct Grüneisen parameter Γ_b, the initial slope of the pressure dependence of the boson-peak frequency ω_b is given by Eq. (2.15) as $\lim_{P\to 0}(\partial\omega_b/\partial P) = \Gamma_b\omega_b/K$, where K is the compression modulus of the glass at zero pressure.

In the present paper, we will take two approaches to describe the thermal expansion in the temperature region corresponding to the boson-peak frequency. The first is to assume a linear variation of the Grüneisen parameter at the boson peak with increasing frequency. This is a two-parameter fit that requires $\Gamma(\omega_b)$ (which not necessarily equals Γ_b, see the fit of vitreous silica) as one parameter and the slope of the Grüneisen parameter at ω_b as the second, see Eq. (2.15).

The second possible fit is to take our model, in which all temperature shift of the excess modes is described by the four parameters n, γ_J, γ_ω, and α_{corr}, too many parameters to be fitted to the data. However, the knowledge of both $\Gamma(\omega_b)$ and the slope $\partial\Gamma(\omega)/\partial\omega$ at ω_b allows to calculate the scaling of $g(\omega_b)/\omega_b^2$ with ω_b. Thus one can determine n from Eq. (2.25), use the approximate form of Eq. (2.21) for γ_J and fit only γ_ω.

This is a compromise because α_{corr} is set to zero without any justification. Nevertheless, such a fit is useful, because it links the measurements to the physical mechanisms of the boson peak. It will at least give some indication of the relative magnitudes of the different contributions discussed above.

1. Vitreous silica

The first example is vitreous silica. The upper part, Fig. 5(a), compares three measurements [52–54] to the heat capacity determined from the inelastic neutron scattering spectrum [54] at 51 K, to show that there is agreement within experimental error. Having asserted this, one can take the measured vibrational spectrum $g(\omega)$ and fit the measured thermal expansion in Fig. 5(b) with an appropriate Grüneisen parameter. Since the thermal expansion is negative, one needs a negative Grüneisen parameter. This shows immediately that the proportionality of the boson-peak frequency to $(1 + P/P_0)^{1/3}$ valid at high pressures does not work at small pressures, because it predicts a positive Grüneisen parameter. This excludes the possibility that the BP shift is fully determined by the nonaffine uncorrelated force effects.

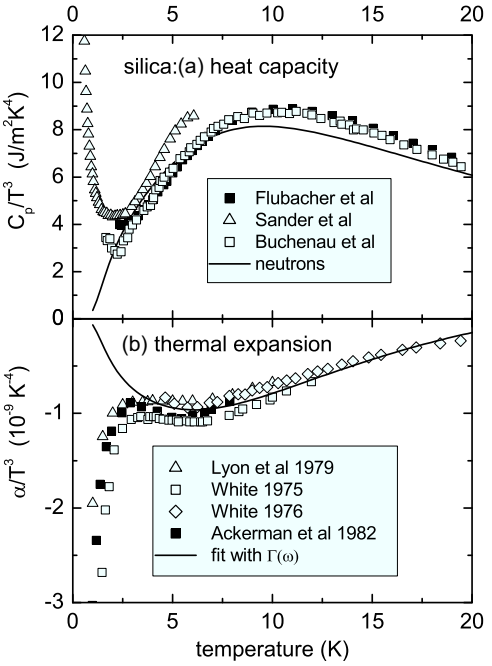

FIG. 5. Low-temperature thermal properties of vitreous silica. (Top) Heat capacity c_p per unit volume, plotted as c_p/T^3, where T is the temperature. Measured data [52–54] are in reasonable agreement with the heat capacity calculated from the vibrational density of states measured by inelastic neutron scattering [54] at 51 K. (Bottom) The volume thermal expansion α, plotted as α/T^3. The measured data [55–58] are fitted in terms of the neutron spectrum at 51 K, attributing a Grüneisen parameter $\Gamma(\omega) = -4.4 + 1.2(\hbar\omega - \hbar\omega_b)$ to the vibrations around the boson-peak frequency $\hbar\omega_b = 4$ meV.

One sees in Fig. 5, top that the peak in α/T^3 is shifted to lower frequency with respect to the peak in c_p/T^3. This shows that the Grüneisen constants of the modes vary. We introduce a frequency-dependent Grüneisen parameter $\Gamma(\omega)$ of the form

$$\Gamma(\omega) = \Gamma(\omega_b) + \Gamma_1(\omega - \omega_b), \tag{4.5}$$

where Γ_1 describes the linear variation of $\Gamma(\omega)$ near the boson peak. The fit in Fig. 5, bottom, required the values $\Gamma(\omega_b) = -4.4$ and $\Gamma_1 = 1.2$ meV^{-1}, as specified in the caption. With this frequency-dependent Grüneisen parameter, we then calculate the thermal expansion coefficient according to Eq. (4.3).

The thermal Grüneisen parameter at the maximum of c_P/T^3 corresponding to the boson-peak frequency is -4.4 (negative, because the thermal expansion in the relevant region is negative). This is not directly Γ_b, because the boson peak is a peak in $g(\omega)/\omega^2$. In order to determine Γ_b, we calculate the peak shift for a small volume change numerically. In this procedure, we find a strong influence of the linear variation of $\Gamma(\omega)$ at ω_b. For silica, we get $\Gamma_b = -10.8$, a much larger negative value than $\Gamma(\omega_b)$.

The reason for this strikingly large difference lies in the behavior of the background of a peak in $g(\omega/)\omega^2$, which initially is a density of states proportional to frequency squared. Note that our slope value of 1.2 meV^{-1} implies that one has a negative Grüneisen parameter of -9.2 at the frequency zero, which gradually goes to zero at about twice the boson-peak

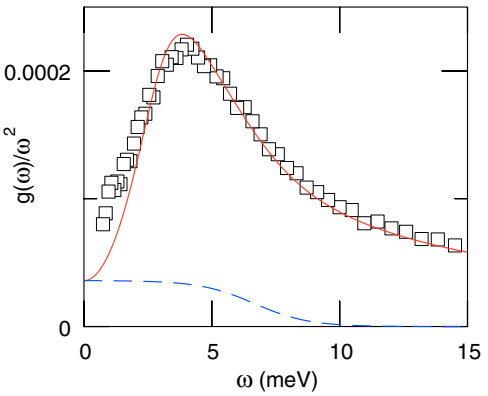

FIG. 6. (Color online) Fit of the reduced vibrational density of states of vitreous silica. Symbols: neutron scattering measurement [54], blue dashed line: Debye part, and red line: sum of Debye part and excess density. Boson peak height and intensity are fitted to the experimental value.

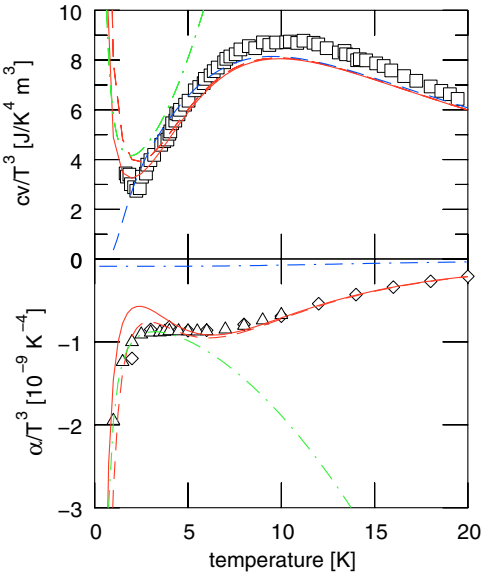

FIG. 7. (Color online) Fit of the low-temperature thermal properties of vitreous silica. (Top) Heat capacity c_p per unit volume, plotted as c_p/T^3. Symbols: measured data [54], red line: values calculated for the fitted spectrum in Fig. 6, dashed red line: values with increased TLS contribution, blue line: values calculated from the measured vibration spectrum, and green dash-dotted line: low-temperature fit [57]. (Bottom) Volume thermal expansion α plotted as α/T^3. Measured data: triangles and diamonds [59]; green dash-dotted line: low-temperature fit [57]; blue dash-dotted line: contribution of the Debye part calculated with the measured low-temperature Grüneisen constant $\gamma_D = -2.29$ [60]; solid red line: sum of total vibrational and TLS contributions; and dashed red line: sum of total vibrational and enhanced TLS contributions.

frequency. The strong frequency dependence of the Grüneisen parameter has a drastic influence on the scaling behavior of $g(\omega_b)/\omega_b^2$, which no longer scales with $1/\omega_b^3$. Instead, the numerical calculation showed a much weaker scaling with $1/\omega_b^{1.3}$. In our model, this would imply a value of $n = 0.93$ to satisfy Eq. (2.25).

Next, we investigate how these findings translate to our description in terms of QLVs. As a first step we fit the reduced VDOS, see Figure 6. Following the procedure outlined above, we choose $n = 1$, use the approximate form of Eq. (2.21) for γ_J, and fit only γ_ω.

Since our model only determines the excess VDOS, $g_{\rm exc}(\omega)$, we add the experimentally known Debye part. There is a problem concerning its high-frequency cutoff. Near the BP frequency, the Ioffe-Regel limit is reached for the sound waves, the modes become strongly intertwined. Level repulsion will affect all the modes strongly. In the approximation of the present model, this means that the modes turn into "high-frequency oscillators." To take this into account, a smooth cutoff was introduced, see the dashed blue line.

As to be expected, the heat capacity calculated for the fitted VDOS (red line) is in good agreement with the measured vibrational part of the specific heat, see Fig. 7, top. The deviation from experiment is similar to the one of the simple quadratic fit (blue line). To include the contributions of the two-level systems (TLS), which dominate c_V below $T \approx 2$ K, we added the term $c_{\rm TLS} = 3.04\ {\rm Jm^{-3}\ K^{-2}}$ determined experimentally [57]. For comparison, we show by the dash-dotted green line the low-temperature fit by Lyon *et al.* [57]. At temperatures around 2 K, this fit indicates a higher number of thermally active modes than in our fit. Such a difference is also observed experimentally for different samples, see Fig. 5. This can be accounted for in our description by increasing the two-level contribution to $c_{\rm TLS} = 3.04\ {\rm Jm^{-3}\ K^{-2}}$ (dashed red line).

Next, we calculate the thermal volume expansion coefficient at low temperatures. We consider only the "affine" effects discussed above. This would give us, in principle, three parameters: γ_ω, γ_J, and n. To reduce the number of parameters, we fix $n = 1$, as indicated from the above, and take $\omega_c = 2.5\omega_B$. We assume that in the considered temperature interval no dramatic effects regarding the mode couplings occur and approximate the coupling partial Grüneisen constant by the Debye expression of Eq. (2.21) $\gamma_J \approx 0.5 - \gamma_D$. The remaining unknown γ_ω, the partial Grüneisen constant of noninteracting modes, we then treat as fit parameter. For $\gamma_\omega = 15$, we get an excellent fit, apart from the lowest temperature, see red line in Fig. 7, bottom. The TLS contribution was taken as $\alpha_{\rm TLS}/T^3 = -1.323$ [57]. Increasing the TLS contribution as before for the specific heat, the fit becomes perfect also at low temperatures (red dashed line). The Debye contribution to the low-temperature volume expansion is nearly negligible (blue dash-dotted line). For comparison, the low-temperature fit of Lyon *et al.* is shown as green dash-dotted line. The fitted value of γ_ω has not too much significance since it would be strongly affected by including correlated nonaffine contributions. Not taking these into account, n is given within a margin of about 30%.

The Grüneisen parameters of the individual modes constituting the BP cannot be readily identified. Instead, we define a frequency dependent Grüneisen parameter $\gamma(\omega)$ by averaging over modes of similar frequency. We define the shift of the modes by

$$\int_0^{\omega} d\omega' g(\omega', P = 0) = \int_0^{\omega+\Delta\omega(P)} d\omega' g(\omega', P). \quad (4.6)$$

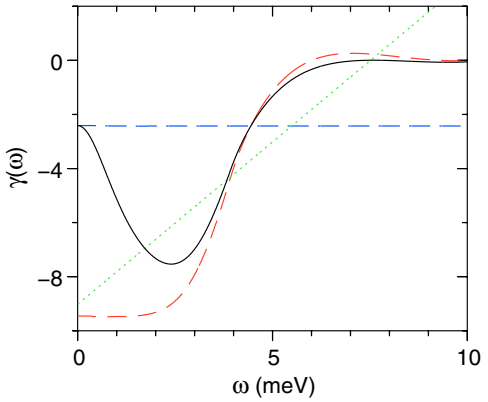

FIG. 8. (Color online) Frequency-dependent Grüneisen constants of SiO_2: of the total spectrum (solid black line), the Debye part (blue dash-dotted line), and the excess spectrum (red dashed line). The experimental fit, Fig. 5, is shown as green dotted line.

This procedure accounts for the net effect of individual modes shifted up and down by pressure and accounts for the conservation of the number of modes. We calculate the mode Grüneisen constants $\gamma(\omega)$ within the context of our description. These refer to the eigenmodes of of our system as opposed to the γ_ω, which describe a frequency independent average shift of the noninteracting modes. The red dashed line in Fig. 8 shows the frequency dependent Grüneisen parameter of the excess modes. At low frequencies, it starts with a constant value of $\gamma(\omega) \approx -9$ that indicates a strengthening of the $g(\omega) \propto \omega^4$ part of the spectrum. The shifting of modes from the higher-frequency part of the BP is reflected in a decrease of the negative value of $\gamma(\omega)$. The experimental fit of Fig. 5 can be seen as a linear approximation (green line). The constant Grüneisen constant of the Debye modes is indicated as blue line. The total frequency-dependent Grüneisen constant is shown in black. It starts at the Debye value and is dominated at higher frequencies by the BP.

2. PMMA

The second example in Fig. 9 is a polymer, polymethylmethacrylate (PMMA). Again, the neutron measurement [62] at 40 K is in reasonable agreement with the measured heat capacity data [61], as shown in Fig. 9(a). The measured thermal expansion [57,58] in Fig. 9(b) is positive and explainable in terms of a single frequency-independent Grüneisen $\Gamma = 2.4$ for all modes comprising the BP. The numerical calculation gives $\Gamma_b = 2.35$, close to $\Gamma(\omega_b)$. This shows that for a weak frequency dependence, one can approximate Γ_b by the value $\Gamma(\omega_b)$, which in turn corresponds to $\Gamma(T)$ at the maximum of c_p/T^3 according to Eq. (4.2). Note that the value $\Gamma = 2.4$ is less than the value for the sound waves (Debye modes) $\gamma_D = 4.25$, reported in Ref. [57]. The approximation of a constant $\Gamma(\omega)$, therefore does not hold at the lowest frequencies.

To check whether our description can reproduce the experimental findings, we employ the same procedure as for vitreous silica. Figure 10 shows that the reduced VDOS of PMMA again can be fitted by a Debye part with a smooth cutoff (blue line) plus our universal BP shape.

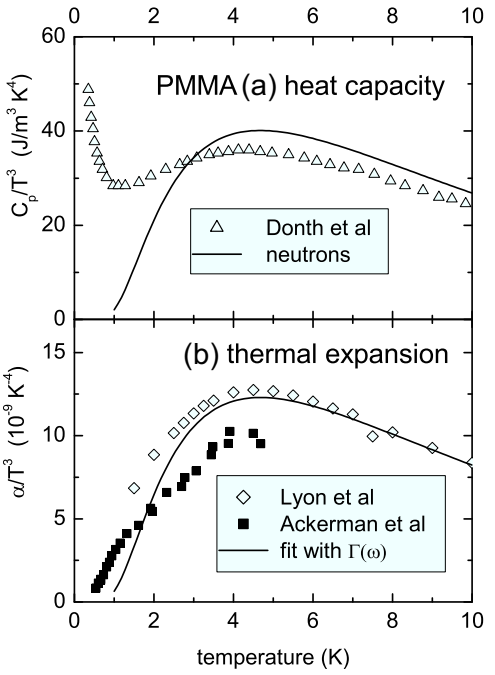

FIG. 9. Low-temperature thermal properties of polymethylmethacrylate (PMMA). (Top) Heat capacity c_p per unit volume, plotted as c_p/T^3, where T is the temperature. Measured data [61] are in reasonable agreement with the heat capacity calculated from the vibrational density of states measured by inelastic neutron scattering [62] at 40 K. (Bottom) The volume thermal expansion α, plotted as α/T^3. The measured data [57,58] are fitted in terms of the neutron spectrum at 40 K with a frequency-independent Grüneisen parameter $\Gamma = 2.4$.

The heat capacity calculated from the fitted VDOS (red line) again is in good agreement with the measured vibrational part of the specific heat, see Fig. 11, top. To include the contributions of the two level systems (TLS), which dominate c_V below $T \approx 2$ K, we added the term $c_{TLS} = 5.28$ Jm^{-3} K^{-2} determined experimentally [57]. For comparison. we also show by the dash-dotted green line the low-temperature fit by Lyon *et al.* [57]. The volume expansion coefficient again

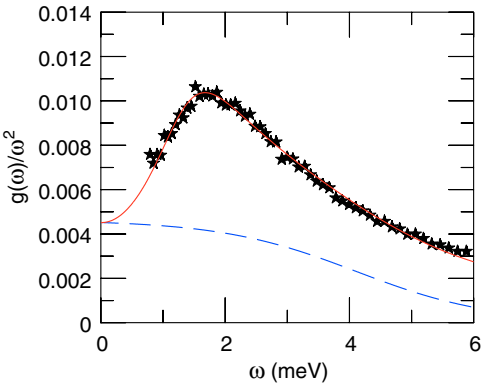

FIG. 10. (Color online) Fit of the reduced vibrational density of states of polymethylmethacrylate (PMMA). Symbols: neutron scattering measurement [62], blue dashed line: Debye part, and red line: sum of Debye part and excess density.

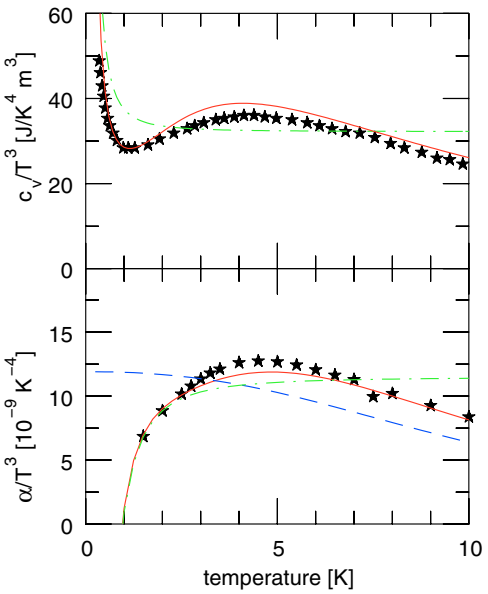

FIG. 11. (Color online) Fit of the low-temperature thermal properties of polymethylmethacrylate (PMMA). (Top) Heat capacity c_p per unit volume, plotted as c_p/T^3. Symbols: measured data [61] and red line: values calculated for the fitted spectrum in Fig. 6 with an added contribution for TLS [57]. For comparison, a low-temperate fit using TLS and Debye contributions [57] is shown (dash-dotted green line). (Bottom) Volume thermal expansion α plotted as α/T^3. Symbols: measured data [57] and blue line: contribution of the Debye part calculated with the measured low-temperature Grüneisen constant $\gamma_D = 4.25$ [57], green line: fit by a sum of tunneling and Debye contributions [57] and red line: sum of tunneling, Debye and BP contributions using one parameter fit $\gamma_\omega = 0.4$, γ_J given by Eq. (2.21).

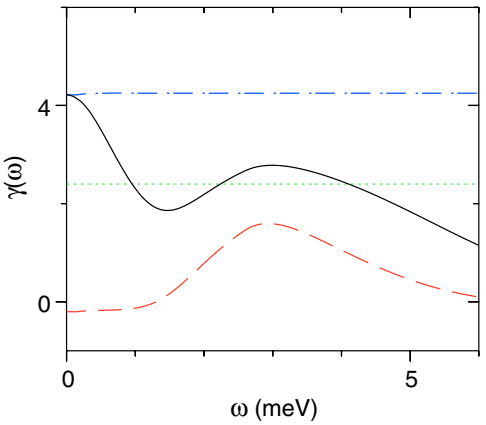

FIG. 12. (Color online) Frequency-dependent Grüneisen constants of the total vibrational spectrum (black solid line) of PMMA, of the Debye part (blue dash-dotted line), and of the excess spectrum (red dashed line). The experimental fit, Fig. 9, is shown as green dotted line.

can be fitted by a single parameter $\gamma_\omega = 0.38\gamma_D$. The fit is slightly improved by a higher value of n than in the silica case and we set it to $n = 2$. This value is, however, not well defined by the fit. For γ_J, we use again the approximate expression, Eq. (2.21). To account for the tunneling systems, we added a term $\alpha_{\rm TLS}/T^3 = -10.56$ [57]. The resulting fit (solid red line) again is in agreement with experiment. Other than in the silica case the vibrational part of the volume expansion is dominated by the Debye contribution (blue dashed line). For comparison, we also show the low-temperature fit by Lyon *et al.* (green dash-dotted line). Figure 12 shows the vibrational Grüneisen parameters. It shows clearly the much higher values of the Debye contribution (blue line) compared to the one of the excess modes (red line). The weighted sum of the two gives the total Grüneisen parameter $\Gamma(\omega)$ (black line). It tends to drop with increasing frequency and shows due to the BP a maximum, that is shifted to higher frequencies compared to the maximum in the scattering intensity. The value fitted directly from experiment, Fig. 9 averages over the low-frequency part.

B. High pressure

In the following, we discuss high-pressure measurements of the boson peak, most of them done with the Raman scattering technique. This has the disadvantage of showing the boson peak at a higher frequency than the one of the true maximum in $g(\omega)/\omega^2$. Hopefully, however, the relative change of the boson-peak frequency should be the same.

1. Vitreous silica

At room temperature and high pressure, the boson-peak frequency of vitreous silica does not decrease, but increases strongly [36] (though with an initial low-pressure increase of nearly zero [63]), following the prediction of Eq. (2.43) with $P_0 = 0.44$ GPa. If this effect were due exclusively to the correlated effect of Eq. (2.43), one would expect with $K = 45$ GPa a positive initial slope of $\Gamma_b = 36$. Instead, one has a strongly negative initial slope. Thus one concludes that the uncorrelated effects dominate the high-pressure behavior in silica, probably due to pressure-induced relaxations, which increase the internal strains and thus increase the linear mode potential terms at the boson peak.

This interpretation is supported by a measurement of the sound velocities in silica at room temperature up to high pressures [64]. Though their pressure dependence is much weaker than the one of the boson peak, they also show an anomalous behavior. Up to a pressure of 3 GPa, they decrease (in accordance with the measured negative Grüneisen parameter of the Debye frequency [57]) and then rise for higher pressures. The initial decrease is limited to the pressure range where no irreversible changes are induced. As soon as the pressures are high enough to cause irreversible changes, the sound velocity after pressure removal remains higher than the initial one. Irreversible structural changes automatically mean increased atomic displacements and in turn enhanced local forces and a larger shift of the BP, expressed by lower P_0 values.

The interpretation is further supported by the properties of densified silica [62], which has a 10% higher Debye frequency and a factor of 1.6 higher boson-peak frequency than normal vitreous silica. Densified silica, obtained by applying a strong pressure at higher temperature (but still well below the glass temperature) and releasing the pressure at room temperature,

is an example that exhibits *only* the irreversible changes. The measurement shows that the irreversible changes have the opposite sign to the reversible ones, but are also much stronger for the boson peak than for the sound waves, with a similar ratio.

2. As_2S_3

In the well-investigated case [39] of As_2S_3, the measurements extend down to rather low pressure. One does not see any indication of a failure of Eq. (2.43) at low pressure, i.e., no indication of a crossover from correlated to uncorrelated force effects. This would indicate the opposite situation to SiO_2, namely, a dominance of the correlated effect and a small contribution by configurational changes.

One can check this conjecture by a direct comparison to the low-temperature data [60]. The high-pressure measurements corroborate again Eq. (2.43) with $P_0 = 0.55$ GPa. The bulk modulus [65] at room temperature is 13 GPa, so one expects $\Gamma_b = 7.8$ from Eq. (2.30). Instead, $\Gamma(T)$ in the boson-peak region is constant and has the much smaller value 1.8. The comparison shows that more than three quarters of the high-pressure effect must be due to uncorrelated forces.

As_2S_3 has a glass temperature of 454 K, not too far above room temperature. Since one expects the relaxational processes to be thermally activated, it is possible that they start at rather low pressure but their trace is not seen in an irreversible remnant.

Nevertheless, since the measurement was done below T_g where no complete recovery to the original state is possible, one should expect some irreversible effects, which should be revealed in a dedicated search. Such a dedicated search would require careful experiments with virgin samples, freshly cooled in a well-defined way from the glass transition. If one repeats the room-temperature experiment several times (as one usually does to see whether one has reproducible results), one cannot expect to see the irreversible part; this should only be visible the first time.

3. B_2O_3

An even larger difference than in As_2S_3 is found in B_2O_3, where the low-temperature expansion data [60] suggest a Γ_b close to zero, while room-temperature high-pressure measurements of the boson peak, interpreted in terms of Eq. (2.43), suggest $P_0 = 0.29$ GPa. With a bulk modulus [66] of 11 GPa, one would expect $\Gamma_b = 11.4$. This example shows again a much stronger pressure dependence of the boson peak in the irreversible high-pressure range, i.e., a clear predominance of the effect of uncorrelated forces at high pressure.

4. Polymers

There are no high-pressure measurements of the boson-peak frequency for PMMA, but for five other polymers [41], which again obey Eq. (2.43). Extrapolated from high pressures, the five polymers have an average value $\Gamma_b = 4.6$ (the lowest value is 3.48) decidedly higher than the value 2.35 extrapolated from the low-temperature measurements. Thus there is little doubt that the uncorrelated term dominates the high-pressure behavior also in the polymers.

V. DISCUSSION

Our results show that, at least for the studied substances, the picture of the BP formed from QLV provides a mechanism of the low-temperature volume expansion as well as the high-pressure shift of the BP and its intensity. For the low-temperature expansion, theory allows for more parameters than one can fit to the data. The parameters can be combined to two effective parameters describing the shift and enhancement of the BP.

All low-frequency vibrational eigenmodes in the glass, including the ones forming the BP are extended. In our interpretation, they are superpositions of local modes, the "oscillators" at the centers of the QLV, and extended sound wavelike modes. The BP is formed by an interaction of the local modes. By this mechanism, a softening of the oscillator modes can even cause a blue shift of the BP. This is contrary to the results of a simplified description in terms of localized vibrations (oscillators) only [67].

In our description, the VDOS of the excess modes increases at the lowest frequencies as $g(\omega) \propto \omega^4$ and above the BP as $g(\omega) \propto \omega$. The initial ω^4 increase is a universal property. Therefore results relating to this frequency range are quite stable. The high-frequency flank of the BP is much more strongly affected by the interaction with a varying number of modes with varying interaction strengths. Although the shape of the BP is largely universal there are slight variations due to anharmonic terms around and above the BP [35]. These deviations from the "universal" shape are effected by pressure. In particular, modes pushed up by a decrease of the ω^4 part, i.e., modes pushed out of the seagull singularity will be moved to the higher-frequency region to conserve the number of vibrational modes. In our calculation, we have strictly conserved the number of modes. How exactly these modes are distributed near and above the BP is beyond our simple description. We have reproduced the low-temperature thermal expansion by a single parameter γ_ω, the Grüneisen coefficient of the local noninteracting modes (the oscillators of the soft potential model). The resulting values of γ_ω are in a reasonable range but it should not be forgotten that they may hide correlated nonaffine contributions or changes of the intermode coupling beyond the simple Debye effect. The message we want to convey is that the description by QLVs reproduces the temperature dependence of the thermal expansion, not what the exact value of the various macroscopic parameters is.

The present work poses several questions. Why does the nonaffine (force) effect seem to be stronger at high pressures or why can we not extrapolate from high to low pressures or vice versa? What is the role of irreversible processes? What is the relative importance of correlated versus uncorrelated effects, i.e., the dependence of $\omega_b(P)$ on P or P^2.

The case of SiO_2 clearly shows a discrepancy between high- and low-pressure properties. At low temperatures, the volume expansion indicates a shift of the "oscillator" frequencies with a Grüneisen parameter comparable to the Debye one and an additional shift by the nonaffine (force) effects discussed in our previous work [35]. The pressure shift of the BP follows the $(P/P_0)^{1/3}$ law predicted for the nonaffine effect at high pressure but is zero or even negative at low pressure. The

positive boson-peak shift on densification allows to associate the high-pressure effect to relaxations.

Also in crystalline quartz at low temperatures, negative expansion and Grüneisen coefficients are found [68,69], but the thermal expansion remains positive at all temperatures. This shows that the strongly negative Grüneisen parameters at and below the boson peak are a specific glass effect. Higher-frequency modes, both in quartz and in vitreous silica, tend to have positive Grüneisen constants [70], which leads to positive expansion coefficients at higher temperatures.

VI. CONCLUSION

The boson peak due to QLV is highly asymmetric. The excess of the inelastic scattering intensity over the Debye intensity (given by the sound waves) increases at low frequencies $\propto\omega^2$ and drops $\propto\omega^{-1}$ above the BP frequency, ω_b. Low-frequency modes are very susceptible to perturbations. A shift of a few vibrational modes in or out of the low-frequency flank strongly affects ω_b, whereas a similar shift on the high-frequency side has much less effect. The dominant effect of pressure on the BP is therefore asymmetrically on the low-frequency side.

We have discussed the various contributions to the shift of the boson peak under an applied pressure. For crystalline lattices, the change of the vibrational density of states is mostly described in the quasiharmonic approximation. The eigenfrequencies are calculated from the harmonic coefficients evaluated for the pressure dependent lattice constants. The Grüneisen constants are given by the change of the harmonic force constants under pressure. This can be written as derivative with respect to strain times strain as function of pressure. In analogy to this, we defined affine Grüneisen parameters that include the effects of uniform changes of distances.

In glasses, such a description is not sufficient. Disorder causes large nonaffine displacements whose effects cannot fully be described by the averaged affine effects. Forces induced by nonaffine displacements cause additional shifts of the boson peak. They lead, in particular, to the high-pressure shift $\propto(P/P_0)^{1/3}$ observed in experiment. The forces can be split into correlated and uncorrelated forces. Correlated forces are due to the elastic polarizability of soft vibrations. They enhance the forces that lead to the creation of the boson peak in the first place. Additionally, pressure can induce new forces uncorrelated to the existing ones. Strong such forces will be induced, e.g., if one crosses the energy barrier between two structural energy minima.

Nonreversibility might be a clue to this, whereas the BP shift due to correlated effects depends on P, the shift by the uncorrelated ones is independent of the sign of P, it only depends on the modulus of the pressure (or pressure squared). For high positive pressure, the two force effects are indistinguishable. Experiments involving negative pressures could lift this ambiguity. The influence of reversible and irreversible local relaxations could be probed by measurements at different temperatures.

In the comparison to experiment, we described four cases where the comparison of the low-pressure boson-peak shifts calculated from low-temperature thermal measurements was much smaller than the value extrapolated from high-pressure measurements. This shows that the high-pressure forces are predominantly uncorrelated to the random forces, which already exist. This suggests that they are mainly due to pressure-induced relaxations.

To avoid future misunderstandings, we want to stress that in the expression $P_0 = 3Kf_0/\Lambda_0$, all quantities refer to the state $P = 0$. Changes with pressure of the compression modulus K largely cancel with the concomitant change of the coupling Λ_0. This explains why even in materials with a large variation of K a constant P_0 may be observed.

Our description is valid for boson peaks, which are caused by disorder. Boson peaks that originate in intrinsic soft modes, also present in a crystalline structure, may have different properties. If disorder and coupling between such modes becomes sufficiently large a "disorder BP" may appear and eventually merge with the intrinsic one.

ACKNOWLEDGMENTS

The authors gratefully acknowledge numerous discussions with D. A. Parshin in the course of our joint work during twenty years. One of us (V.L.G.) wants to acknowledge the hospitality of the Forschungszentrum Jülich where part of this work was done.

[1] *Amorphous Solids. Low Temperature Properties*, edited by W. A. Phillips (Springer-Verlag, Berlin, 1981).
[2] A. Heiming, W. Petry, J. Trampenau, M. Alba, C. Herzig, H.R. Schober, and G. Vogl, Phys. Rev. B **43**, 10948 (1991).
[3] V. N. Sagaev, E. N. Smelyanskaya, V. G. Plotnichenko, V. V. Koltashev, A. A. Volkov, and P. Pernice, J. Non-Cryst. Solids **248**, 141 (1999).
[4] M. A. Ramos, S. Vieira, F. J. Bermejo, J. Dawidowski, H. E. Fischer, H. Schober, M. A. González, C. K. Loong, and D. L. Price, Phys. Rev. Lett. **78**, 82 (1997).
[5] R. M. Lynden-Bell and K. H. Michel, Rev. Mod. Phys. **66**, 721 (1994).
[6] H. Shintani and H. Tanaka, Nat. Mater. **7**, 870 (2008).
[7] D. A. Parshin, H. R. Schober, and V. L. Gurevich, Phys. Rev. B **76**, 064206 (2007).
[8] J. Fabian and P. B. Allen, Phys. Rev. Lett. **77**, 3839 (1996).
[9] H. R. Schober, J. Phys.: Condens. Matter **16**, S2659 (2004).
[10] W. Schirmacher, G. Diezemann, and C. Ganter, Phys. Rev. Lett. **81**, 136 (1998).
[11] T. S. Grigera, V. Martin-Mayor, G. Parisi, and P. Verrocchio, J. Phys.: Cond. Matter **14**, 2167 (2002).
[12] S. N. Taraskin, J. J. Ludlam, G. Natarajan, and S. R. Elliott, Phil. Mag. B **82**, 197 (2002).
[13] Y. M. Beltukov and D. A. Parshin, JETP Lett. **93**, 598 (2011).
[14] B. Schmid and W. Schirmacher, Phys. Rev. Lett. **100**, 137402 (2008).

[15] W. Schirmacher *et al.*, Phys. Stat. Sol. C **5**, 862 (2008).
[16] W. Schirmacher, J. Non-Cryst. Solids **357**, 518 (2011).
[17] S. N. Taraskin, Y. L. Loh, G. Natarajan, and S. R. Elliott, Phys. Rev. Lett. **86**, 1255 (2001).
[18] A. I. Chumakov *et al.*, Phys. Rev. Lett. **106**, 225501 (2011).
[19] G. Monaco and V. M. Giordano, Proc. Natl. Acad. Sci. USA **106**, 3659 (2009).
[20] V. N. Novikov and N. V. Surovtsev, Phys. Rev. B **59**, 38 (1999).
[21] E. Duval, A. Mermet, and L. Saviot, Phys. Rev. B **75**, 024201 (2007).
[22] V. L. Gurevich, D. A. Parshin, and H. R. Schober, Phys. Rev. B **67**, 094203 (2003).
[23] M. A. Ramos and U. Buchenau, Phys. Rev. B **55**, 5749 (1997).
[24] U. Buchenau, Yu. M. Galperin, V. L. Gurevich, and H. R. Schober, Phys. Rev. B **43**, 5039 (1991).
[25] U. Buchenau, Yu. M. Galperin, V. L. Gurevich, D. A. Parshin, M. A. Ramos, and H. R. Schober, Phys. Rev. B **46**, 2798 (1992).
[26] V. G. Karpov, M. I. Klinger, and F. N. Ignatiev, Zh. Eksp. Teor. Fiz. **84**, 760 (1983) [Sov. Phys. JETP **57**, 439 (1983)].
[27] M. A. Il'in, V. G. Karpov, and D. A. Parshin, Zh. Eksp. Teor. Fiz. **92**, 291 (1987) [Sov. Phys. JETP **65**, 165 (1987)].
[28] U. Buchenau, H. M. Zhou, N. Nücker, K. S. Gilroy, and W. A. Phillips, Phys. Rev. Lett. **60**, 1318 (1988).
[29] B. B. Laird and H. R. Schober, Phys. Rev. Lett. **66**, 636 (1991); H. R. Schober and B. B. Laird, Phys. Rev. B **44**, 6746 (1991).
[30] A. A. Maradudun, E. W. Montroll, G. H. Weiss, and I. P. Ipatova, *Solid State Physics*, Suppl. 3 (Academic Press, New York, 1971).
[31] P. H. Dederichs, C. Lehmann, H. R. Schober, A. Scholz, and R. Zeller, J. Nucl. Mater. **69/70**, 176 (1978).
[32] H. R. Schober, J. Non-Cryst. Solids **357**, 501 (2011).
[33] F. Faupel, W. Frank, M.-P. Macht, H. Mehrer, V. Naundorf, K. Rätzke, H. R. Schober, S. S. Sharma, and H. Teichler, Rev. Mod. Phys. **75**, 237 (2003).
[34] M. I. Klinger, Phys. Rep. **492**, 111 (2010).
[35] V. L. Gurevich, D. A. Parshin, and H. R. Schober, Phys. Rev. B **71**, 014209 (2005).
[36] R. J. Hemley, C. Meade, and H.-K. Mao, Phys. Rev. Lett. **79**, 1420 (1997).
[37] M. Yamaguchi, T. Nakayama, and T. Yagi, Physica B **263-265**, 258 (1999); **81**, 1 (1978).
[38] J. D. Boyer, J. C. Lasjaunias, R. A. Fisher, and N. E. Phillips, J. Non-Cryst. Sol. **55**, 413 (1983).
[39] K. S. Andrikopoulos, D. Christofilos, G. A. Kourouklis, and S. N. Yannopoulos, J. Non-Cryst. Solids **352**, 4594 (2006).
[40] K. Niss, B. Begen, B. Frick, J. Ollivier, A. Beraud, A. Sokolov, V. N. Novikov, and C. Alba-Simionesco, Phys. Rev. Lett. **99**, 055502 (2007).
[41] L. Hong, B. Begen, A. Kisliuk, C. Alba-Simionesco, V. N. Novikov, and A. P. Sokolov, Phys. Rev. B **78**, 134201 (2008).
[42] T. Deschamps, C. Martinet, D. de Ligny, J. L. Bruneel, and B. Champagnon, J. Chem. Phys. **134**, 234503 (2011).
[43] T. C. Penna, L. F. O. Faria, J. R. Matos, and M. C. C. Ribeiro, J. Chem. Phys. **138**, 104503 (2013).
[44] F. Leonforte, J. Non-Cryst. Solids **357**, 552 (2011).
[45] H. R. Schober and C. Oligschleger, Phys. Rev. B **53**, 11469 (1996).
[46] H. R. Schober and G. Ruocco, Phil. Mag. **84**, 1361 (2004).
[47] G. Leibfried and N. Breuer, *Point Defects in Metals I, Springer Tracts in Modern Physics Vol. 81*, edited by G. Höhler and E. A. Niekisch (Springer-Verlag, Berlin, Heidelberg, New York, 1978).
[48] F. Leonforte, R. Boissière, A. Tanguy, J. P. Wittmer, and J.-L. Barrat, Phys. Rev. B **72**, 224206 (2005).
[49] D. Srivastava and S. K. Sarkar, Phys. Rev. B **85**, 024206 (2012).
[50] H. R. Schober, J. Nucl. Mater. **126**, 220 (1984).
[51] H. Boettger, *Principles of the Theory of Lattice Dynamics* (Physik Verlag, Weinheim, 1983).
[52] P. Flubacher, A. J. Leadbetter, J. A. Morrison, and B. P. Stoicheff, J. Phys. Chem. Solids **12**, 53 (1959).
[53] H. v. Löhneysen, H. Rüsing, and W. Sander, Z. Phys. B **60**, 323 (1985).
[54] U. Buchenau, M. Prager, N. Nücker, A. J. Dianoux, N. Ahmad, and W. A. Phillips, Phys. Rev. B **34**, 5665 (1986).
[55] G. K. White, Phys. Rev. Lett. **34**, 204 (1975).
[56] G. K. White, Cryogenics **16**, 487 (1976).
[57] K. G. Lyon, G. L. Salinger, and C. A. Swenson, Phys. Rev. B **19**, 4231 (1979).
[58] D. A. Ackerman and A. C. Anderson, Phys. Rev. Lett. **49**, 1176 (1982).
[59] G. K. White, J. A. Birch, and M. H. Manghnani, J. Non-Cryst. Solids **23**, 99 (1977).
[60] G. K. White, S. J. Collocott, and J. S. Cook, Phys. Rev. B **29**, 4778 (1984).
[61] M. Beiner, S. Kahle, S. Abens, E. Hempel, S. Höring, M. Meissner, and E. Donth, Macromolecules **34**, 5927 (2001).
[62] U. Buchenau, A. Wischnewski, M. Ohl, and E. Fabiani, J. Phys.: Condens. Matter **19**, 205106 (2007).
[63] T. Deschamps, C. Martinet, D. R. Neuville, D. de Ligny, C. Coussa-Simon, and B. Champagnon, J. Non-Cryst. Solids **355**, 2422 (2009).
[64] Ch.-Sh. Zha, R. J. Hemley, H.-K. Mao, Th. S. Duffy, and C. Meade, Phys. Rev. B **50**, 13105 (1994).
[65] M. P. Brassington, J. Miller, and G. A. Saunders, Phil. Mag. B **43**, 1049 (1981).
[66] M. Grimsditch and L. M. Torell, in *Dynamics of Disordered Materials*, edited by D. Richter, A. J. Dianoux, W. Petry, and J. Teixeira (Springer, Berlin, 1989), p. 196.
[67] V. Hizhnyakov, A. Laisaar, J. Kikas, A. Kuznetsov, V. Palm, and A. Suisalu, Phys. Rev. B **62**, 11296 (2000).
[68] T. H. K. Barron, J. F. Collins, T. W. Smith, and G. K. White, J. Phys. C **15**, 4311 (1982).
[69] G. A. Lager, J. D. Jorgensen, and F. J. Rotella, J. Appl. Phys. **53**, 6751 (1982).
[70] Q. Williams, R. J. Hemley, M. B. Kruger, and R. Jeanloz, J. Geophys. Res. **98**, 22157 (1993).